

Optimization of a two-phase transverse flux switched reluctance motor with an outer rotor

MARIAN ŁUKANISZYN, MARCIN KOWOL, JANUSZ KOŁODZIEJ

*Opole University of Technology
Prószkowska 76, 45-758 Opole
e-mail: m.lukaniszyn@po.opole.pl*

(Received: 25.01.2012, revised: 13.06.2012)

Abstract: This paper presents optimization results for a two-phase, modular transverse flux switched reluctance motor (TFSRM) with an outer rotor. In particular, the main disadvantage of the considered motor structure, that is the zero starting torque in some rotor positions, is eliminated by construction optimization. A numerical model of the motor developed in the Flux3D program is coupled with a Matlab-based evolutionary algorithm for optimization of construction parameters of the magnetic circuit. The elaborated algorithm is also connected with a database to limit the computation costs. Three objective functions are taken into account for the motor integral parameter improvement. The fundamental role of a type of an optimization criterion function is comparatively analyzed and a new effective criterion function is introduced.

Key words: transverse flux switched reluctance motor, outer rotor, optimization

1. Introduction

Transverse flux motors (TFMs) have recently attracted remarkable interest both from the academia and various industrial environments [2, 4, 5]. The low-speed motor is characterized by a high ratio of the electromagnetic torque to its volume [12, 15, 17], leading immediately to various high-torque transmission-free applications, to mention electric wind generators [2], electric (and hybrid) drives [10] and in-wheel drives [11, 14]. Reduction of the ripple torque is certainly welcome in the above high-torque implementations, but it is vital in modern control and robotics applications [3] or for an aero-engine shaft-line-embedded starter/generator [7, 8].

Nowadays, the design of electromechanical convertors is often reduced to the problem of optimization, e.g. in terms of maximization of the average torque and/or reduction of torque pulsations. To this end, various optimization methods and criterion functions have been used [6, 9, 12, 18, 19]. In this paper, the problem of evolutionary optimization of the magnetic circuit for a two-phase TFSRM (Figures 1 and 2) is analyzed.

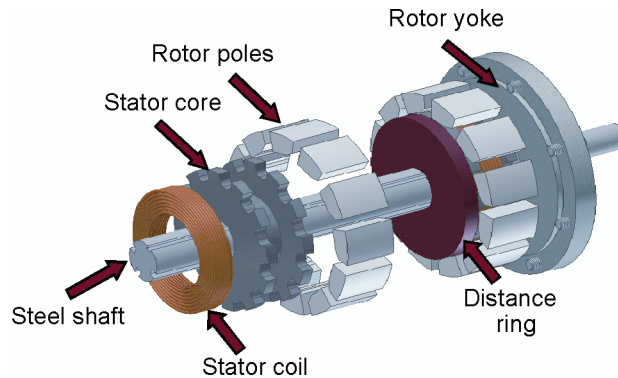


Fig. 1. Schematic view of single-phase module of two-phase TFSRM and its units

In the previous papers by the authors [12-14, 16, 17], principles of operation of the three-module motor, performance prediction, an effective three-dimensional analysis of the magnetic field distribution and full optimization of the magnetic circuit for the three-module TFSRM have been presented. Specifically, the influence of the selection of various sets of three-module TFSRM construction parameters on the electromagnetic torque and its pulsations has been comparatively examined. The simulation results were in good agreement with experimental data obtained from the prototype motor, which confirmed the usefulness of the computational approach. Similar topology of the motor with segmented rotor has been considered by Mecrow research group [1, 7, 8]. Machines of this type have been used for small stepper motors, with the magnetic circuit produced from solid steel [1].

In order to additionally improve electromechanical parameters and efficiency of TFSRMs, the new construction of a two-module reluctance motor has been designed by the authors. This work is an extension of the related topics presented in the area in Refs. [13, 14, 16, 17]. This paper analyzes selected constructions of two-module TFSRMs. This motor structure has the main defect – the start torque of the motor is equal to zero for specific rotor positions. This paper offers a new solution to this problem.

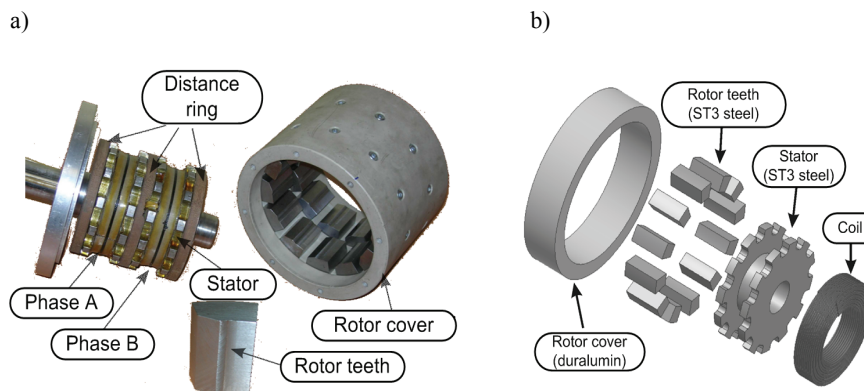


Fig. 2. Prototype two-module TFM(a) and its units (b)

An effective tool for the purpose is the 3D FEM and an adequate modeling environment is the Flux3D program. The program is coupled with the Matlab package, that contains the evolutionary algorithms, as the main optimization tool. It should be stressed that the employed modeling and optimization tools enable the avoidance of constructing and verifying a number of physical motor prototypes, which could be very expensive.

The prototype motor structure is shown schematically in Figure 2. The considered motor consists of two identical modules in which the stators are shifted by fifteen mechanical degrees between each other. The rotor modules are placed symmetrically. Each module has twelve teeth and includes one phase of the winding in the shape of a solenoidal coil. The rotor and its teeth are made of solid iron. The modules are separated from each other with non-magnetic inserts. The main specifications for the motor are given in Table 1.

Table 1. Specifications for TFM

Supply voltage	$U_n = 24 \text{ V}$
Rated current	$I_n = 12 \text{ A}$
Rotational speed	300 rpm
Winding	Two-phase
Number of turns per coil	130
External diameter of rotor	$r_m = 158 \text{ mm}$
External diameter of stator	$r_s = 103.5 \text{ mm}$
Air gap	$\delta = 0.5 \text{ mm}$
External length of rotor	$l_m = 148 \text{ mm}$

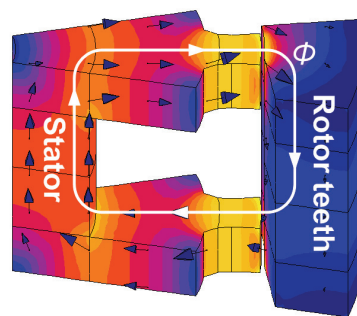


Fig. 3. Simplified topology of magnetic flux circulation

The analysis presented in this work was carried out for a small, low-voltage (12 and 24 V), two-phase TFSRM with an outer rotor. The number of turns of one phase coil is equal to 130 and the rated current value in the calculation is assumed to be 12 A. A simplified topology of the circulation of the main flux is shown in Figure 3, which illustrates the operation principle of the machine. The motor operates as a two-phase machine with a position feedback loop. The motor is supplied from a DC source through a two-pulse electric inverter, see Figure 4. Control of the motor is reduced to supplying the phases with a rectangular current waveform

according to the sequence A, B, A. Conduction of any phase results in adequate positioning of the rotor with respect to the stator (the teeth are aligned). Since the rotor sectors are shifted between each other, the successive connection of the phases causes the rotor to rotate. The connection of the successive phases is triggered by the signals from two transoptor sensors located in the external module. The sensors co-operate with a light-reflecting disc mounted onto an inner wall of the rotor.

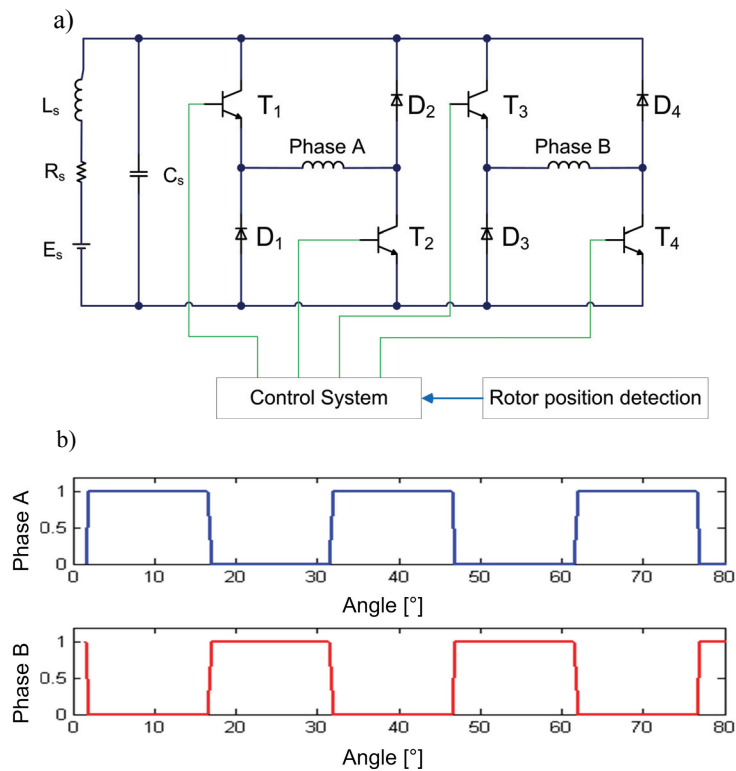


Fig. 4. The half-bridge (“H”) TFSRM power converter (a) and current waveforms (b)

It is worth mentioning that we have constructed the basic two-module prototype according to the state-of-the-art and using our long-years of experience, including results of our previous, three-module prototype constructions [14, 16, 17].

2. Numerical model

3D FEM is a necessary numerical tool for an analysis of special-construction motors like TFSRM [12-14]. A numerical model of the motor is based on the Flux3D program [12]. A simplifying assumption is introduced into the calculations that no magnetic couplings occur between the modules, which is justified by separation of the modules with the nonmagnetic

inserts of an appropriate width. The assumption enables to limit the calculations to a single module only and, taking additional account for the symmetry conditions in the motor, to 1/48 of the motor volume (see Fig. 5). A structure of the motor module with a discretization mesh for the numerical model is depicted in Figure 6.

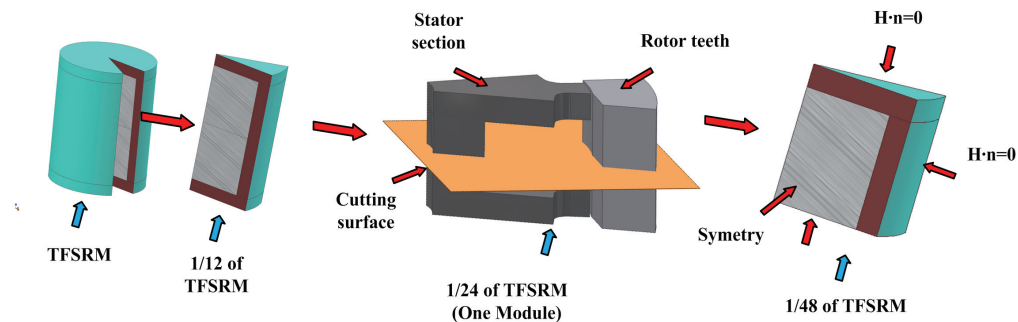


Fig. 5. Construction of TFSRM of numerical model of module with boundary conditions

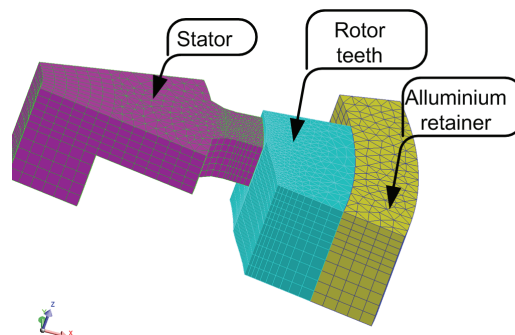


Fig. 6. TFSRM module with a discretization mesh

The electromagnetic torque is calculated by the virtual work method as a derivative of the magnetic coenergy with respect to the rotation angle between the rotor and stator. The rotation of the rotor vs. the stator is modeled by the sliding surface method [12, 14, 17]. The magnetic hysteresis and eddy currents are omitted in the calculations and a constant current density is assumed in the whole cross-section of the coils.

A detailed description of the numerical model for the motor can be found in References [12, 17]. In the comparative analysis, a useful torque pulsation factor is employed

$$\varepsilon = \frac{T_{\max} - T_{\min}}{2T_{av}} \cdot 100\%, \tag{1}$$

where T_{\max} , T_{\min} , T_{av} denote the maximum, minimum and average values of the electromagnetic torque, respectively.

3. Two-phase TFSRM optimization by means of an evolutionary algorithm

In this paper, minimization of certain criterion functions is numerically performed by making use of an evolutionary algorithm (EA), being a generalization of a genetic algorithm [6, 9]. EA is known to have a (very) low probability of being stuck in a local minimum.

Construction optimization of the TFSRM is performed under assumptions of constant volume and constant external diameter of the motor module. The optimization tool, that is the EA available in the Matlab environment, is coupled with the Flux3D program used to design the magnetic circuit. A general block diagram of the optimization process is presented in Figure 7.

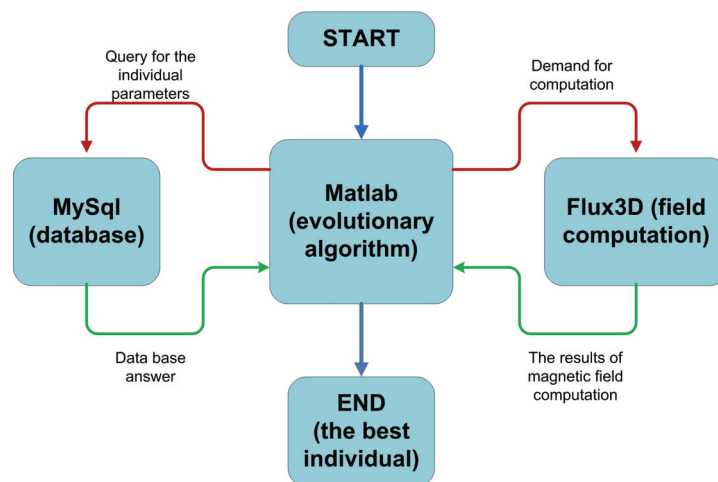


Fig. 7. General diagram of optimization process

Since field models are characteristic of a high computational burden, in particular for 3D FEM, the optimization algorithm is extended, in a well-known manner, to include a database. The database is used to store the data of individuals and the calculated electromagnetic torque with the accuracy of the first decimal point, which has been found sufficient (Note: The use of more sophisticated solutions [6, 9, 15] has not been found necessary here). Prior to each field calculation cycle, the data base is searched to determine whether field calculations have already been made for the generated individual. In the case that such an individual has been found in the database, the magnetic field calculations are omitted. This enables to essentially save computation times as the execution times both for the save operation and searching the database are negligible when compared to the torque calculation times.

A cross-section of the module of the TFSRM is illustrated in Figure 8. With a constant air gap $\delta = 0.5$ mm, the following construction parameters are assumed to be the decision variables in the optimization task: α_1 , α_2 , β , r_{x1} , r_{x2} , r_{x3} , r_{x4} , which are arranged in the vector \underline{x} . Those parameters mainly reflect a selection of a range of the stator poles and a shape of the rotor poles. The limitation to only 7 variables results from the earlier analysis of influence of

specific construction parameters on electromechanical properties [12, 13, 17]. In fact, the remaining construction parameters of the motor have been found to affect the average electromagnetic torque only slightly. It is also worth mentioning that due to the specific construction of the motor the angle γ is justified to be assumed constant (regarding the induction saturation effect in the rotor poles).

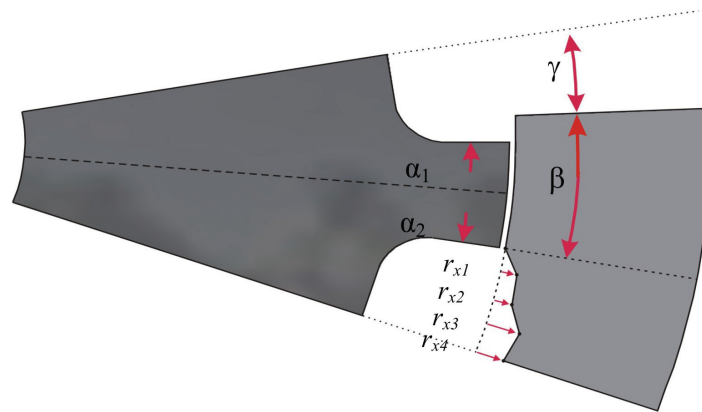


Fig. 8. Cross-section of module of TFSRM

The main target of optimization for the two-phase motor is obtaining the extension of a range of positive values of the electromagnetic torque produced by the motor. A wider range of angles for positive values of the electromagnetic torque guarantees the start of the motor for all rotation positions between the rotor and stator.

4. Calculation results for various criterion functions

Using the evolutionary optimization algorithm, a number of computer simulation runs have been performed. EA is set to operate on 20 individuals per population and a number of generations equal to 100 is assumed as a stop condition for the algorithm. The first optimization task is pursuing the maximum extension of a range of positive values of the electromagnetic torque produced by the motor. For such an optimization task, the criterion or objective function can be proposed as

$$\max_{\underline{x} \in X} \{ \xi_1(\underline{x}) = l_u(\underline{x}) \} \tag{2}$$

$$X \subset R^7,$$

where $l_u(\underline{x})$ is the range of positive values of the electromagnetic torque produced by the motor.

The EA procedure was run five times for various initial conditions and same parameter values for the genetic operators. The highest obtained value of the criterion function was $\xi_{1\max} = 40.0$. In this case, the obtained angle extension of a range of positive values of the elec-

tromagnetic torque produced by the motor is equal to 5°. Unfortunately, a side effect of the above optimization is that the average electromagnetic torque is reduced almost 2 times, with the external construction parameters (r_m , l_m) and the supply conditions retained. Another side effect is that pulsations of the electromagnetic torque are increased by some 18%.

The best solution, that is according to (2) is now additionally presented in terms of plots of Figure 9 of the electromagnetic torque vs. rotor rotation angle.

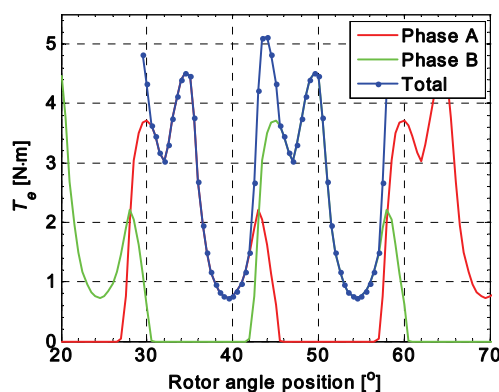


Fig. 9. Electromagnetic torque vs. rotor rotation angle after optimization as in (2)

Taking into account the side effects of application of the objective function ξ_1 , in the next stage of our study a new criterion ξ_2 is proposed. The interest is to find a construction solution for which minimal value of the electromagnetic torque (especially start torque) would be maximized. In this case, the criterion function can be assumed as:

$$\max_{\underline{x} \in X} \{ \xi_2(\underline{x}) = T_{\min}(\underline{x}) \},$$

$$X \subset R^7, \quad (3)$$

Several runs of the EA procedure have been performed for the criterion (3). For the best obtained solution, the electromagnetic torque is plotted in Figure 10. The obtained solution enables to reduce the pulsations factor (1) of the electromagnetic torque by some 44%. However, the average electromagnetic torque is lower by some 26% (see Tab. 2).

The criterion (2) has led to the extension of a range of positive values of the electromagnetic torque produced by the motor at the cost of increased pulsations and reduction of the electromagnetic torque. On the other hand, the criterion (3) has provided the reduction of pulsations of the electromagnetic torque by more than 44%, with lower range of positive torque values. Therefore, in the next stage of our study, we seek for a sort of a compromise between the high average electromagnetic torque and a range of its positive values, the requirement represented by an appropriate weighting of the criteria (2) and (3). Now, a new, „compromise” objective function can be proposed as:

$$\max_{x \in X} \{ \xi_3(x) = wT_{av}(x) + (1-w)l_u(x) \}$$

$$X \subset R^7,$$
(4)

where $w \in [0, 1]$ is the weighting coefficient, T_{av} is the average torque.

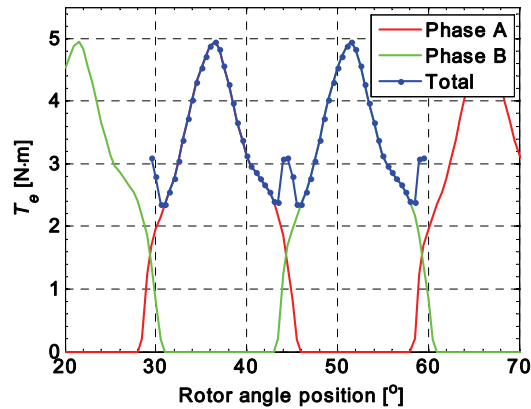


Fig. 10. Electromagnetic torque vs. rotor rotation angle after optimization as in (3)

The criterion given in Equation (4) is a single point on the Pareto front, i.e. the front generated by all possible values of w for the two objective function components [6, 9]. Thus, the objective/fitness function (4) provides a simple realization of the evolutionary design in multi-criterial optimization. The criterion (4) covers a plethora of optimization tasks, ranging from the high-average torque ones as in (3) to the wider range of angles for positive values of the electromagnetic torque as in (2). Selection of a specific weighting coefficient depends on a specific TFSRM application. The results for (a sort of) the ‘best’ solution are presented in Figure 11 ($w = 0.5$). The solution was obtained from the plethora of numerical experiments [12].

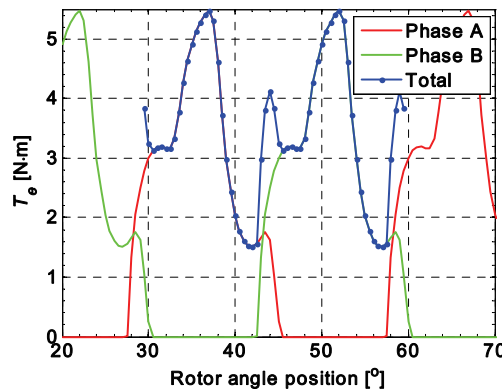


Fig. 11. Electromagnetic torque vs. rotor rotation angle after optimization as in (4)

In this case, the obtained extension of a range of positive values of the electromagnetic torque produced by the motor is equal to 3°. Now, the average electromagnetic torque is lower only by some 24% as compared to the initial motor prototype, with the external construction parameters (r_m , l_m) and the supply conditions retained. On the other hand, the pulsations of the electromagnetic torque are also lower by some 15%.

All the best solutions, that is according to (2), (3), and (4), are now additionally compared in terms of the integral parameters for the two-phase TFSRM before and after optimization (see Table 2). Optimization according to the criterion (4) shows flexibility as compared to all the other optimization cases and is an additional advantage here.

Table 2. Integral parameters for TFM before and after optimization with switch-overs ($I = 12$ A)

	Before optimization	After optimization			Change [%]		
		ξ_1	ξ_2	ξ_3			
T_{max} [N·m]	6.22	5.12	4.94	5.47	-18	-21	-12
T_{min} [N·m]	0	0.73	2.35	1.50	---	---	---
T_{av} [N·m]	4.66	2.79	3.43	3.50	-40	-26	-24
ε [%]	66.73	78.75	37.71	56.49	18	-44	-15
l_u [°]	15	19	17.5	18	27	17	20

5. Basic vs. optimized physical models of the motor

Taking into account our specific, high-torque motor application, a new, optimized TFSRM prototype was constructed according to the criterion ξ_2 solution presented in the above Table 2. Taking account for the simplifying assumptions made at the modeling stage as well as some manufacture inaccuracy occurred in providing the specific air gap and the complicated shape of the rotor tooth, the quality improvement for the optimized vs. basic prototypes is really impressive.

For additional illustration of the final effect, Figure 12 presents plots of the calculated/measured electromagnetic torques (produced by one phase without switch-overs) vs. rotor position for the constructed prototype motor, for several values of the current. The high modeling accuracy is self-explanatory.

6. Conclusions

This paper has presented various possible solutions to the problem of optimization of construction parameters of two-module TFSRM making use of a combination of an evolutionary algorithm and 3D FEM. An optimum design enables the determination of a specific tooth shape and can provide a nonzero start torque for the motor under design, without making its costly prototype(s). Thus, the main contribution of the paper is that possible zero starting torque

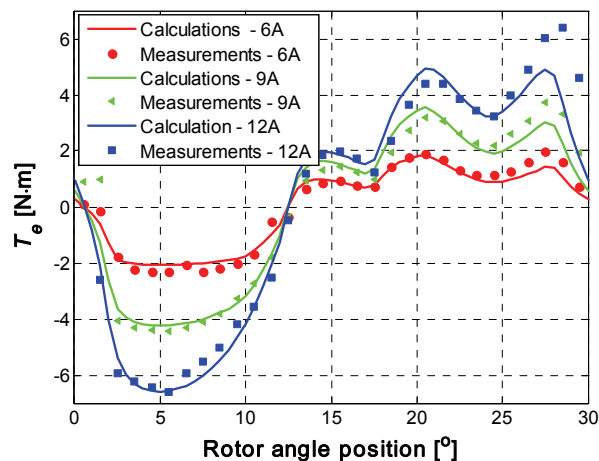


Fig. 12. Electromagnetic torque vs. rotor rotation angle for one phase of optimized TFSRM prototype without switch-overs (calculations vs. measurements)

in some rotor position is eliminated by construction optimization. In addition to advantageous effects of the evolutionary algorithm, the performance of the optimization process depends largely on a type of a criterion function used. The criterion function can be formulated in various ways for the same construction optimization task. The cost function (4) is a new flexible and effective criterion function proposed for the purpose, with a range of values of the weighting coefficient covering various optimal tasks, depending on specific applications of the motor.

The optimum construction design has been effectively applied in a new TFSRM prototype. Electromechanical parameters of the optimized prototype motor have been found to be very close to the theoretically calculated figures and much better than those for the basic, unoptimized prototype used as a reference. This illustrates the versatility of the numerical model and the optimization procedure employed.

References

- [1] Amreiz H.M., Mecrow B.C., Wiener C., *Switched reluctance machines with simple hoop windings*. IEE Power Electronics, Machines and Drives Conf., Publ. 487: 522-526 (2002).
- [2] Arshad W.M., Thelin P., Bäckström T., Sadarangani C., *Use of transverse-flux machines in a free-piston generator*. IEEE Trans. Ind. Appl. 40(4): 1092-1100 (2004).
- [3] Babazadeh A., Parspour N., Hanifi A., *Transverse flux machine for direct drive robots: Modelling and analysis*. IEEE Conference on Robotics, Automation and Mechatronics, Singapore, 1: 376-380 (2004).
- [4] Babazadeh A., Parspour N., *Analysis of shifted transverse flux reluctance motor*. International Conference on Optimization of Electrical and Electronic Equipment, Bravos, Romania, pp. 53-58 (2004).
- [5] Dubois M.R., Dehlinger N., Polinder H., Massicotte D., *Clawpole transverse-flux machine with hybrid stator*. International Conference on Electrical Machines (ICEM), Chania, Crete Island, Greece, PSA, pp. 4-11 (2006).

- [6] De Jong K.A., *Evolutionary computation: a unified approach*. MIT Press, Cambridge MA (2006).
- [7] Hall R., Jack A.G., Mecrow B.C., Mitcham A.J., *Design and initial testing of an outer rotating segmented rotor switched reluctance machine for an aero-engine shaft-line-embedded starter/generator*. IEEE International Conference on Electric Machines and Drives, pp. 1870-1877 (2005).
- [8] El-Kharashi E.A., Mecrow B.C., Finch J.W., Jack A.G., *Switched reluctance motors with segmental rotors*. IEE Proceedings, Electric Power Applications 149(Issue: 4): 245-254 (2002).
- [9] Fonseca C.M., Gandibleux X., Hao J.K., Sevaux M., (Eds.), *Evolutionary Multi-Criterion Optimization*. Proc. 5th International Conference, EMO 2009, Nantes, France, Series: Lecture Notes in Computer Science 5467 (2009).
- [10] Isastia V., Bellucci M., *A new configuration of a TFPM machine for a wheel motor*. ICEM 2004, Cracow 1: 139-140 (2004).
- [11] Kastinger G., *Design of a novel transverse flux machine*. ICEM 2002, Brugge, (conf. CD) (2002).
- [12] Kołodziej J., *Analysis dynamic and steady transverse flux motor work states*. (in Polish). Ph.D. thesis, Opole University of Technology, Opole (2011).
- [13] Kołodziej J., Kowol M., Łukaniszyn M., *Modelling and optimization of the two-module switched reluctance motor*. Przegląd Elektrotechniczny (Electrotechnical Survey) 11:100-105 (2011).
- [14] Kowol M., Łukaniszyn M., Latawiec K., *Modeling and construction optimization of modular TFM with outer rotor*. Electrical Engg. 92(3): 111-118 (2010).
- [15] Laurenceau J., Meaux M., Montagnac M., Sagaut P., *Comparison of Gradient-Based and Gradient-Enhanced Response-Surface-Based Optimizers*. AIAA Journal 48(5): 981-994 (2010).
- [16] Łukaniszyn M., Kowol M., *Influence of construction modification on the electromechanical parameters of the modular reluctance motor with outer rotor*. (in Polish), Przegląd Elektrotechniczny (Electrotechnical Survey) 82(11): 43-45 (2006).
- [17] Łukaniszyn M., Kowol M., *Optimization of magnetic circuit of a modular reluctance motor with an outer rotor*. Poznań University of Technology Academic Journals, Electrical Engineering, pp. 157-166 (2007).
- [18] Viorel I., Jufer M., Crivii M., Viorel A., *Scaling procedure applied to the transverse flux motor*. ICEM 2004, Cracow (Poland), pp. PS2-20, (2004).
- [19] Wang X., Du J., Ren N., Liu Z., Tang R., *Optimization of stator structure of transverse flux motor*. Journal of Iron and Steel Research International 13(Supplement 1): 466-470 (2006).